Cryogenic Liquid Rocket Engine Test Bench Fault-Tolerant Control System: Cooling System Application

C. Sarotte * **J. Marzat** * **H. Piet Lahanier** * **M. Galeotta** ** **G. Ordonneau** ***

* *DTIS, ONERA, Université Paris-Saclay, F-91123 Palaiseau, France*
** *CNES, DLA, Paris, France*
*** *DPE, ONERA, Université Paris-Saclay, F-91123 Palaiseau, France*

Abstract: A nonlinear fault-tolerant control strategy relying on quantitative physics-based models for a cryogenic combustion bench operation is proposed in this paper. The aim is to improve the reliability of a cryogenic bench operation in the transients and to allow to converge to a wider range of operating points. The fault detection is performed with residual-based methods. The residual is generated by an unknown input observer with an unscented transformed which also allows to reconstruct the unknown input. Then the goal is to provide a fault-tolerant system reconfiguration mechanism with a control law which compensates for the estimated actuator additive faults to maintain the overall system stability. For that purpose we use a model predictive control method on an equivalent system with the reconstructed unknown input. An error feedback and a fault compensation control law is designed in order to minimize an infinite horizon cost function within the framework of linear matrix inequalities. The model and the estimation part were validated on real data from Mascotte test bench (ONERA/CNES), and the reconfiguration control law was validated in realistic simulations.

Keywords: Actuator fault accommodation, cryogenic system, fault-tolerant control, nonlinear observer, nonlinear control, LMI, discrete-time system, model predictive control

1. INTRODUCTION

Monitoring engines and test benches is a major challenge in the development and integration of new propulsion systems for rockets, including reusable ones (Wu (2005)). A conventional control design for such complex systems may result in an unsatisfactory performance, or even instability, in the event of malfunctions in actuators, sensors or other system components. The objectives are to design efficient, fast and reliable approaches to detect faults of various magnitudes (Betta and Pietrosanto (2000)). Then, if a minor component and/or instrument fault is detected by the model-based Fault Detection and Isolation (FDI) approaches as presented in Yin et al. (2016), non-shutdown actions have to be defined to maintain the overall system current performances close to the desirable ones and preserve stability conditions (see Yang et al. (2010)). For that reason, it is required to perform a reconfiguration (see Ioannou and Sun (1996)) of the engine using Fault tolerant control systems (FTCS). Active FTC Systems firstly detect and estimate faults, then, the second step is to achieve a steady-state tracking of the reference input by compensating the fault as in Theilliol et al. (2008). For that purpose, FDI methods have been developed to evaluate failures and take a decision using all available information with the help of explicit or implicit models (Zhong et al. (2018)). The most common model-based approach for FDI makes use of observers to generate residuals as presented in Ding (2008). Those FDI methods assume that the mathematical model used is representative of the system dynamics (Gertler (2013)).

To tackle the problem of unknown disturbances, a simple class of Unknown input observer (UIO) (Darouach et al. (1994)) for linear systems with unknown inputs has been developed. It consists in a coordinate system transformation that decouples the disturbance effect on the system outputs. An UIO is used to estimate the unknown state of the system independently of the unknown input. In the case of nonlinear systems one of the developed techniques is to linearize and design an Extended unknown input observer (EUIO) as described in Witczak (2007). However as for Extended Kalman filters, in those methods the state distribution is approximated by a Gaussian Random Variable (GRV) which is then propagated analytically through the "first-order" linearization of the nonlinear system. Those linearizations imply the definition of a steady state reference and can introduce large errors in the true posterior distribution, which may lead to sub-optimal performance and sometimes divergence of the filter as presented in Wan and Van Der Merwe (2000). For those reasons, Unscented Observers (UO) based on the unscented transform have been developed. UO are based on a parameterization which captures the mean and covariance information and at the same time permits the direct propagation of the information through an arbitrary set of nonlinear equations which overcome the previous limitations of extended observers (Józefowicz et al. (2011)). In the case of actuator failures, it is necessary to

be able to handle emergency situations that can affect a system performance. Linear quadratic regulators (LQR) or linear Model Predictive Control (MPC) have been widely used in different industry (Maciejowski (1999), Abbas-Turki et al. (2007)). However, for engine applications, nonlinear effects may affect the controller performances and a nonlinear approach may allow to consider a wider range of operating points (Mhaskar et al. (2006)). For that reason, a nonlinear MPC may be used (Magni et al. (2003)). The MPC approach provides a framework with the ability to handle, among other issues, multi-variable interactions, input constraints, and optimization requirements. The development and the performance evaluation of the FTC methods should rely on real measurements (Johnson (1996)). For that purpose, this work is partly based on the exploitation of real data from the Mascotte test bench developed at ONERA (Vingert et al. (2015)). It is therefore necessary to have a model of the bench and its current instrumentation to make a first validation of the approaches using a simulation, then validate the results on experimental data. The obtained measurements will also allow updating and adapting the simulation models as well as validating by identification the engine characteristics on off-line tests as carried out in our previous work (Sarotte et al. (2018)). Section 2 consists in the description of the considered system, then a design of a nonlinear model-based FTCS is proposed in order to compensate for an additive actuator failure (Figure 1). The FDI part of the FTCS is composed of an Unscented unknown input observer (UUIO) as developed by Józefowicz et al. (2011). An extension of Poursafar et al. (2010) approach for nonlinear control of discrete-time systems is developed for fault tolerant control applications. This extension is composed a nonlinear model predictive control based on the resolution of Linear matrix inequalities (LMI) and a fault compensation system in the case of an additive actuator failure. A second UUIO allows to reconstruct the fault and to design the fault compensation system. This method has been validated on realistic simulations of a cryogenic combustion test bench cooling circuit. The faults were simulated for several valve closing profiles.

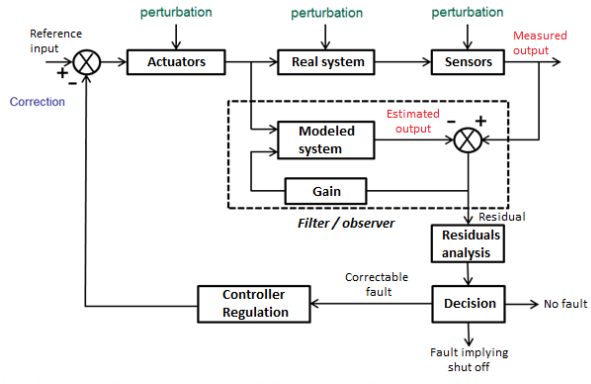

Fig. 1. Active FTCS closed-loop

2. SYSTEM DESCRIPTION

In this section we denote:

- $\dot{m}$, the mass flow rate (kg/s),
- ρ, the density (kg/m^3),
- S, the surface (m),
- c, the velocity of sound (m/s),
- P, the pressure (Pa),
- D, the orifice diameter (m),
- D_h, the hydraulic diameter (m),
- L the length (m),
- μ the dynamic viscosity (Pa.s),
- V, the volume (m^3),
- d_t, the time step (s).

Subscripts

- e, for input,
- s, for output,
- 1, for the cavity 1,
- 2, for the cavity 2,
- a, for the augmented state.

The flow is assumed to stay monophasic and incompressible. We assume that the fluid flow velocity is small in comparison to the velocity of sound in cavities. The model of this part of the cooling circuit is then (for more details see Sarotte et al. (2018)):

$$\begin{cases} \dfrac{\partial \dot{m}_{2e}}{\partial t} = \theta_1 \dot{m}_{2e}^{\frac{7}{4}} - \theta_2 \Delta P \\ \dfrac{\partial P_2}{\partial t} = -\theta_3 \Delta \dot{m} \end{cases} \tag{1}$$

$$\theta_1 := -0.316 \left(\frac{4}{\pi D \mu}\right)^{-\frac{1}{4}} \frac{L}{D_h} \frac{1}{2\rho V}, \theta_2 := \frac{S^2}{V}, \theta_3 := \frac{c^2}{V}$$

The parameter θ_1 must be identified since the distance L is unknown. We can assume here that the density and the viscosity remain constant for the considered pressures and temperature ranges. The system can be transformed into an equivalent discrete-time state space system with an Euler explicit scheme. The system considered is then:

$$\begin{cases} X_{k+1} = f(X_k, U_k) + E d_k + w_k \\ Y_{k+1} = C X_{k+1} + v_{k+1} \end{cases} \tag{2}$$

$$X_k := \begin{bmatrix} \dot{m}_{2e,k} \\ P_{2,k} \end{bmatrix}, Y_k := P_{2,k}, U_k := P_{1,k}, d_k := \dot{m}_{2s,k}$$

Where $\dot{m}_{2e}$ is the cavity 2 input mass flow rate, P_2 is the cavity 2 pressure, P_1 is the cavity 1 pressure and $\dot{m}_{2s}$ is the cavity 2 unknown output mass flow rate. $X_k \in \mathbb{R}^2$ is the state vector, $Y_k \in \mathbb{R}$ is the measured output, $U_k \in \mathbb{R}$ is known input, $d_k \in \mathbb{R}$ is the unknown input, $E \in \mathbb{R}^2$ the unknown input distribution matrix and $C^T \in \mathbb{R}^2$ the output distribution matrix. The model presented here allows to determine the evolution of the ferrules cooling circuit output pressure and input mass flow rate. It is now possible to model their evolution during the motor transients. The model was tested off-line with real measurements of a Mascotte campaign as inputs. Those trials last 60 seconds. The evolution of the pressure and mass flow rate dynamics is well reconstituted (Table 1).

Table 1. Relative errors of the pressure model

	Total (%)	Transient (%)	steady-state (%)
Pressure	5.44	8.01	0.31
Input mass flow rate	3.31e-5	4.97e-5	6.17e-8

3. UNSCENTED UNKNOWN INPUT OBSERVER

The first step is to design an unscented unknown input observer to estimate the state in the presence of unknown inputs. We want to find a parameterization which captures the mean and covariance information while at the same time permitting the direct propagation of the information through an arbitrary set of nonlinear equations. This can be accomplished by generating a discrete distribution having the same first and second moments, where each point in the discrete approximation can be directly transformed (see Wan and Van Der Merwe (2000)). Given a n-dimensional Gaussian distribution having covariance P, we can generate a set of $O(n)$ points having the same sample covariance from the columns of the matrices $\pm\sqrt{2P}$. This set of points is zero mean, but if the original distribution has mean $\bar{X}$, then adding $\bar{X}$ to each of the points yields a symmetric set of $2n+1$ points having the desired mean and covariance. To choose a matrix square root a Cholesky decomposition is used. One can use this methodology to derive a filtering algorithm. The augmented state vector composed of the state and the process noise is defined as:

$$X_{a,k|k} := [X_k{}^T w_k{}^T]^T$$

this augmented vector has a covariance matrix:

$$P_{a,k|k} = \begin{bmatrix} P_{k|k} & P_{x,w,k|k} \\ P_{w,x,k|k} & Q_k \end{bmatrix}$$

Where Q_k is the covariance of w_k and R_k is the covariance of v_k. The previous transformation is then used on the Sigma points from $X_{a,k|k}$:

$$\chi_{i,k|k} := X_{a,k|k} \pm \sqrt{(n+\kappa)P_{a,k|k}}$$
$$\chi_{0,k|k} := X_{a,k|k}$$

κ is a scaling parameter which may be chosen equal to 2 in the case of Gaussian distribution. To evaluate the set of the transformed set of Sigma points in spite of the presence of an unknown input, one can write:

$$d_k = H(Y_{k+1} - C(f(X_k, U_k) + w_k) - v_{k+1}) \quad (3)$$

A necessary condition for the existence of a solution is $\text{rank}(CE) = \text{rank}(E)$. A particular solution is then:

$$H = ((CE)^T(CE))^{-1}(CE)^T \quad (4)$$

Then the transformed set of Sigma points are evaluated for each of the 0 to $2n$ points by:

$$\chi_{i,k+1|k} := \bar{f}(\chi_{i,k|k}, U_{k+1}, k) + \bar{E}Y_{k+1} + \breve{w}_k$$

where $\bar{f} = Tf$, $T = I_n - EHC$ and n the dimension of the state. And $\breve{w}_k = Tw_k - EHv_{k+1}$. The predicted mean is computed as:

$$\hat{X}_{k+1|k} = \frac{1}{n+\kappa}(\kappa\chi_{0,k+1|k} + \frac{1}{2}\sum_{i=1}^{2n}\chi_{i,k+1|k})$$

The predicted covariance is then computed as:

$$P_{k+1|k} = \frac{1}{n+\kappa}(\kappa(\chi_{0,k+1|k} - \hat{X}_{k+1|k})(\chi_{0,k+1|k} - \hat{X}_{k+1|k})^T$$
$$+ \frac{1}{2}\sum_{i=1}^{2n}(\chi_{i,k+1|k} - \hat{X}_{k+1|k})(\chi_{i,k+1|k} - \hat{X}_{k+1|k})^T) + Q_k$$

To complete the design of the filter, the equivalent statistics for the innovation sequence and the cross correlation must be determined. The observation model gives:

$$\mathcal{Y}_{i,k+1|k} = C\chi_{i,k+1|k} + v_{k+1}$$

Then the mean observation is:

$$\hat{Y}_{k+1|k} = \frac{1}{n+\kappa}(\kappa\mathcal{Y}_{0,k+1|k} + \frac{1}{2}\sum_{i=1}^{2n}\mathcal{Y}_{i,k+1|k})$$

The measurements covariance matrix is determined from:

$$P_{yy,k+1|k} = (\kappa(\mathcal{Y}_{0,k+1|k} - \hat{Y}_{k+1|k})(\mathcal{Y}_{0,k+1|k} - \hat{Y}_{k+1|k})^T +$$
$$\frac{1}{2}\sum_{i=1}^{2n}(\mathcal{Y}_{i,k+1|k} - \hat{Y}_{k+1|k})(\mathcal{Y}_{i,k+1|k} - \hat{Y}_{k+1|k})^T)\frac{1}{n+\kappa} + R_k$$

If the disturbances $\breve{w}_k$ and v_k are uncorrelated, the cross correlation matrix is:

$$P_{xy,k+1|k} = (\kappa(\chi_{0,k+1|k} - \hat{X}_{k+1|k})(\mathcal{Y}_{0,k+1|k} - \hat{Y}_{k+1|k})^T$$
$$+ \frac{1}{2}\sum_{i=1}^{2n}(\chi_{0,k+1|k} - \hat{X}_{k+1|k})(\mathcal{Y}_{i,k+1|k} - \hat{Y}_{k+1|k})^T)\frac{1}{n+\kappa}$$

The updated equations are then:

$$K_{k+1} = P_{xy,k+1|k}P_{yy,k+1|k}^{-1} \quad (5)$$
$$\hat{X}_{k+1|k+1} = \hat{X}_{k+1|k} + K_{k+1}(Y_{k+1} - \hat{Y}_{k+1|k}) \quad (6)$$
$$\hat{P}_{k+1|k+1} = P_{k+1|k} - K_{k+1}P_{yy,k+1|k}K_{k+1}{}^T \quad (7)$$

The gain matrix K_{k+1} is chosen to minimize the variance of the state estimation error. The estimation period used on real measurements is fixed to 0.001 seconds. The state estimation error ($e_k = X_k - \hat{X}_k$) is taken as a residual. We then compare the UUIO to an EUIO on the basis of Mascotte test bench real data (see Table 2).

Table 2. Relative errors of the pressure and input mass flow rate estimations

Model		Total (%)	Transient (%)	steady-state (%)
Pressure	UUIO	8.02e-3	1.24e-2	5.07e-3
(Pa)	EUIO	6.71e-3	1.85e-2	2.87e-3
Mass flow rate	UUIO	1.51	2.46	0.10
(kg/s)	EUIO	2.15	6.42	0.41

The unknown input is reconstructed from (3). To validate the result, the unknown input reconstruction is compared to the cavity 2 output mass flow rate measurements available for this trial. Results are reported in Figure 2 and Table 3 and show a correct convergence after the transient phase.

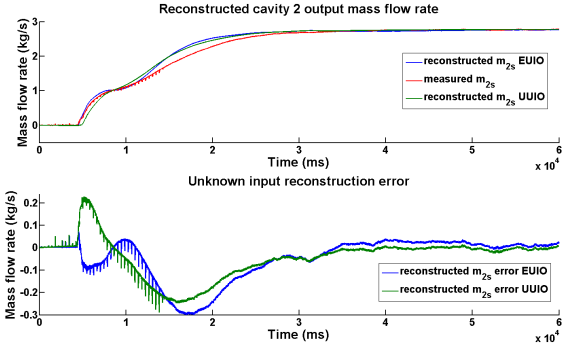

Fig. 2. Unknown input reconstruction

Table 3. Relative error of the output mass flow rate reconstruction

Model		Total (%)	Transient (%)	steady-state (%)
Output mass flow rate (kg/s)	UUIO	1.44	3.14	4.94e-2
	EUIO	2.16	4.98	0.41

It appears that UUIO estimation and fault reconstruction performances are higher than the EUIO ones for the mass flow rate estimation and equivalent for the pressure estimation. Those performances in the transient are satisfying even if a deviation appears at the beginning of the trial, since the feeding valve is not directly opened, but the mass flow rate information is not needed at that time. The offset in the steady-state part of the trial is reduced.

4. NONLINEAR CONTROL FOR LIPSCHITZ SYSTEMS WITH ERROR FEEDBACK AND FAULT COMPENSATION

In this part, the fault reconstruction expression (3) is used to write the system under a new form where the only unknown input is an additive actuator failure. Then, in order to annihilate the actuator fault effect on the system, another UUIO is used to estimate the fault magnitude, the estimated state at the instant k is then denoted $\hat{X}_{c,k}$ and the estimation error $e_{c,k}$. A control law has then to compensate the fault and is computed such that the faulty system is as close as possible to the nominal one. The new system for control purposes is thus:

$$\begin{aligned} X_{k+1} &= (I_n - EHC)f(X_k, U_k) + EHCX_k \\ &\quad + (I_n + EHC)w_k + (EH + C)v_k - EHv_{k+1} + Bf_{ak} \end{aligned} \tag{8}$$

We consider the following system:

$$\begin{cases} X_{k+1} = AX_k + BU_k + \tilde{f}(X_k, U_k) + Bf_{ak} + \tilde{w}_k \\ Y_{k+1} = CX_{k+1} + v_k \end{cases} \tag{9}$$

with $\tilde{f} := (I_n - EHC)(f(X_k, U_k) - X_k) - BU_k$, $\tilde{w}_k = \bar{w}_k + (EH + C)v_k$, $A := I_n$ and $B := [\,0\ 1\,]^T$. Where $X_k \in \mathbb{R}^2$ is the state vector, $Y_k \in \mathbb{R}$ is the measured output, $U_k \in \mathbb{R}$ is the known input and $C^T \in \mathbb{R}^2$ the output distribution matrix, $f_{ak} \in \mathbb{R}$ is the actuator additive fault.

We define $\zeta_k := [\,\eta_k\ e_{c,k}\,]^T$, with $e_{c,k} = \hat{X}_{c,k} - X_k$ the estimation error, $\eta_k = X_k - \overline{X}_k$ the reconfiguration error and $\overline{X}_k$ the state reference. The reference state dynamics can be generated as:

$$\overline{X}_{k+1} := A\overline{X}_k + B\overline{U}_k + \tilde{f}(\overline{X}_k, \overline{U}_k) + \tilde{w}_k$$

with $\overline{U}_k$ a user-defined reference input, which can be for example a reference trial sequence. We then have:

$$\begin{aligned} \zeta_{k+1} &= \begin{bmatrix} A & 0 \\ 0 & K_{k+1}C \end{bmatrix} \zeta_k + \begin{bmatrix} B \\ 0 \end{bmatrix} \Delta U_k + \begin{bmatrix} B \\ 0 \end{bmatrix} f_{ak} \\ &\quad + \begin{bmatrix} I \\ 0 \end{bmatrix} (\tilde{f}(X_k, U_k) - \tilde{f}(\overline{X}_k, \overline{U}_k)) \end{aligned} \tag{10}$$

with $\Delta U_k := U_k - \overline{U}_k$. We can simplify the notation as:

$$\zeta_{k+1} = \mathcal{A}\zeta_k + \mathcal{B}(\Delta U_k + f_{ak}) + \mathcal{C}\Phi_k(X_k, U_k, \overline{X}_k, \overline{U}_k) \tag{11}$$

with $\mathcal{A} := \begin{bmatrix} A & 0 \\ 0 & K_{k+1}C \end{bmatrix}$, $\mathcal{B} := \begin{bmatrix} B \\ 0 \end{bmatrix}$ and $\mathcal{C} := \begin{bmatrix} I \\ 0 \end{bmatrix}$ and $\Phi_k := \tilde{f}(X_k, U_k) - \tilde{f}(\overline{X}_k, \overline{U}_k)$. Φ_k is locally Lipschitz for the cooling system application since $f(X_k, U_k)$ is locally Lipschitz on a compact set $\mathcal{S}_{X_{inf}, X_{sup}, U_{inf}, U_{sup}}$. The considered mass flow rates and pressures are bounded by thermomechanical constraints, $X \in [X_{inf}; X_{sup}]$ and $U \in [U_{inf}; U_{sup}]$. We consider a control law of the following form:

$$\Delta U_k := G\zeta_k - \mathcal{B}^+\mathcal{B}\hat{f}_{ak} \tag{12}$$

The fault $\hat{f}_{ak}$ is estimated from the following unknown input reconstruction scheme:

$$\hat{f}_{ak} = \tilde{H}(Y_{k+1} - C(\tilde{f}(X_k, U_k) + \tilde{w}_k) - v_{k+1}) \tag{13}$$

with $\tilde{H} = ((CB)^T(CB))^{-1}(CB)^T$. We consider the following minimization problem with respect to $\Delta U(\cdot)$ of the infinite horizon cost function:

$$J_k := \sum_{i=0}^{\infty} \zeta_{k+i}^T S \zeta_{k+i} + \Delta U_{k+i}{}^T O \Delta U_{k+i} \tag{14}$$

subject to $\zeta_{k+i} \in \bar{\zeta}$, $\Delta U_{k+i} \in \bar{\mathbb{U}}$ with $i \geq 0$, $\bar{\zeta}$ and $\bar{\mathbb{U}}$ compact subsets of $\mathbb{R}^4$ and $\mathbb{R}$; S and O positive definite weighting matrices. We choose the following Lyapunov candidate function: $V_k := \zeta_k^T P \zeta_k$. If V_k is a Lyapunov function ensuring the stability of the resulting closed-loop then (see Poursafar et al. (2010)):

$$J_k \leq \zeta_k^T P \zeta_k \leq -\gamma \tag{15}$$

with γ a positive scalar and regarded as an upper bound of the objective (14).

Lemma (Poursafar et al. (2010)): *Let M, N be real constant matrices and P be a positive matrix of compatible dimensions. Then:*

$$M^T P N + N^T P M \leq \epsilon M^T P M + \epsilon^{-1} N^T P N \tag{16}$$

holds for any $\epsilon > 0$.

Theorem: Consider the discrete-time system (11) with control input (12) at each time k. We define $V_k = \gamma \zeta_k^T X^{-1} \zeta_k$ a Lyapunov function satisfying (17), where $X > 0$ and Y are obtained from the solution of the following optimization problem with variables γ, α, X, Y and $Z := X[H\ G]^T$. The state-feedback matrix G in the control law that minimizes the upper bound γ of the objective function J_k is then given by $G := YX^{-1}$, with

$$V_{k+1} - V_k \leq -(\zeta_k{}^T S \zeta_k + \Delta U_k{}^T O \Delta U_k) \tag{17}$$

$\min_{\gamma, \alpha, X, Y} \gamma$ subjects to

$$\begin{bmatrix} -X & * & * & * & * \\ \sqrt{1+\epsilon}(\mathcal{A}X + \mathcal{B}Y) & -X & * & * & * \\ \sqrt{(1+\frac{1}{\epsilon})WZ} & 0 & -\alpha I & * & * \\ S^{1/2}X & 0 & 0 & -\gamma I & * \\ O^{1/2}Y & 0 & 0 & 0 & -\gamma I \end{bmatrix} \leq 0, \tag{18}$$

Where $*$ stands for symmetric terms in the matrix. And

$$\begin{bmatrix} -I & * \\ \zeta_k & -X \end{bmatrix} \leq 0. \tag{19}$$

Proof: The linear quadratic function V_k has to satisfy (17) then:

$$(\mathcal{A}\zeta_k + \mathcal{B}(\Delta U_k + f_{ak}) + \mathcal{C}\Phi_k)^T P \quad (20)$$
$$(\mathcal{A}\zeta_k + \mathcal{B}(\Delta U_k + f_{ak}) + \mathcal{C}\Phi_k) - {\zeta_k}^T P \zeta_k$$
$$\leq -({\zeta_k}^T S \zeta_k + \Delta {U_k}^T O \Delta U_k)$$

Defining the function $g(\zeta_k, \Delta U_k, f_{ak})$ as

$$g(\zeta_k, \Delta U_k, f_{ak}) = (\mathcal{A}\zeta_k + \mathcal{B}(\Delta U_k + f_{ak}))^T P \quad (21)$$
$$(\mathcal{A}\zeta_k + \mathcal{B}(\Delta U_k + f_{ak})) + (\mathcal{A}\zeta_k + \mathcal{B}(\Delta U_k + f_{ak}))^T P(\mathcal{C}\Phi_k)$$
$$+ (\mathcal{C}\Phi_k)^T P(\mathcal{A}\zeta_k + \mathcal{B}(\Delta U_k + f_{ak})) + (\mathcal{C}\Phi_k)^T P(\mathcal{C}\Phi_k)$$

and applying the Lemma, the upper bound of $g(\zeta_k, \Delta U_k, f_{ak})$ becomes

$$g(\zeta_k, \Delta U_k, f_{ak}) \leq (1+\epsilon)(\mathcal{A}\zeta_k + \mathcal{B}(\Delta U_k + f_{ak}))^T P \quad (22)$$
$$(\mathcal{A}\zeta_k + \mathcal{B}(\Delta U_k + f_{ak})) + (1+\epsilon^{-1})(\mathcal{C}\Phi_k)^T P(\mathcal{C}\Phi_k)$$

Consider

$$P \leq \lambda_{max} I \leq \mu I \quad (23)$$

where λ_{max} is the maximum eigenvalue of P and μI is a design parameter corresponding to the upper bound of the maximum eigenvalue of P.

$$g(\zeta_k, \Delta U_k, f_{ak}) \leq (1+\epsilon)(\mathcal{A}\zeta_k + \mathcal{B}(\Delta U_k + f_{ak}))^T P \quad (24)$$
$$(\mathcal{A}\zeta_k + \mathcal{B}(\Delta U_k + f_{ak})) + (1+\epsilon^{-1})\mu(\mathcal{C}\Phi_k)^T(\mathcal{C}\Phi_k)$$

Since Φ_k is Lipschitz we have:

$${\Phi_k}^T \mathcal{C}^T \mathcal{C} \Phi_k \leq [{\eta_k}^T \Delta {U_k}^T] W^T \mathcal{C}^T \mathcal{C} W [\eta_k \Delta U_k]^T \quad (25)$$

Then

$$g(\zeta_k, \Delta U_k, f_{ak}) \leq (1+\epsilon)(\mathcal{A}\zeta_k + \mathcal{B}(\Delta U_k + f_{ak}))^T P \quad (26)$$
$$(\mathcal{A}\zeta_k + \mathcal{B}(\Delta U_k + f_{ak}))+$$
$$(1+\epsilon^{-1})\mu[{\eta_k}^T \ \Delta {U_k}^T] W^T \mathcal{C}^T \mathcal{C} W [\eta_k \ \Delta U_k]^T$$

We then have:

$${\zeta_k}^T S \zeta_k + \Delta {U_k}^T O \Delta U_k - {\zeta_k}^T P \zeta_k \quad (27)$$
$$+ (1+\epsilon)(\mathcal{A}\zeta_k + \mathcal{B}(\Delta U_k + f_{ak}))^T P$$
$$(\mathcal{A}\zeta_k + \mathcal{B}(\Delta U_k + f_{ak}))+$$
$$(1+\epsilon^{-1})\mu[{\eta_k}^T \ \Delta {U_k}^T] W^T \mathcal{C}^T \mathcal{C} W [\eta_k \ \Delta U_k]^T \leq 0$$

Considering the following error feedback control:

$$\Delta U_k = G\zeta_k - \mathcal{B}^+ \mathcal{B} \hat{f}_{ak} \quad (28)$$

The previous equation is rewritten as:

$${\zeta_k}^T (S + G^T O G - P + (1+\epsilon)(\mathcal{A} + \mathcal{B}G)^T P(\mathcal{A} + \mathcal{B}G)$$
$$+ (1+\epsilon^{-1})\mu[H^T \ G^T] W^T \mathcal{C}^T \mathcal{C} W [H \ G]^T)\zeta_k \leq 0 \quad (29)$$

Which is satisfied if:

$$S + G^T O G - P + (1+\epsilon)(\mathcal{A} + \mathcal{B}G)^T P(\mathcal{A} + \mathcal{B}G) \quad (30)$$
$$+(1+\epsilon^{-1})\mu[H^T \ G^T] W^T \mathcal{C}^T \mathcal{C} W [H \ G]^T \leq 0$$

We then denote: $X := \gamma P^{-1}$, $X > 0$, $Y := GX$, $\alpha := \gamma\mu^{-1}$, $Z := X[H \ G]^T$. Applying Schur complements give the LMI (18). We also have:

$$-X + \alpha I \leq 0 \quad (31)$$

in order to verify (23), where $*$ stands for symmetric terms in the matrix. And

$$\begin{bmatrix} -I & * \\ \zeta_k & -X \end{bmatrix} \leq 0 \quad (32)$$

to ensure (15).

□

Table 4. Deviations of the simulated pressure and input mass flow rate from references - UUIO-MPC

Control simulation	Pressure (%)	Input mass flow rate (%)
Fault 1 abrupt shift high amplitude	0.17	2.82e-3
Fault 2 slow shift high amplitude	8.77e-2	8.51e-3
Fault 3 abrupt shift flow amplitude and slow shift high amplitude	0.14	3.54e-3

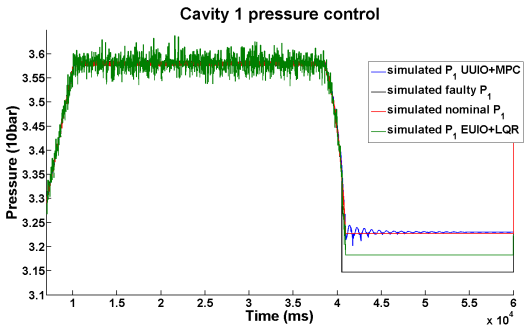

Fig. 3. Pressure and mass flow rate control - Carins simulator - UUIO+MPC

The faulty system was simulated with Carins (CNES simulator), a closing valves profile was imposed at the input of the cooling circuit. The aim of this simulation is to see if the controller is able to stabilize the closed-loop system after the detection. When the fault is detected the system switches to the FTCS. This FTCS is composed of: a FDI part, a first UUIO for fault detection purposes as well as unknown input reconstruction and residual analysis algorithms; a fault compensator, a second UUIO for the rewritten system to estimate and compensate for the fault; a MPC to ensure the system stability and convergence to a reference trajectory. This system has been tested on three sets of failures, see Table 4. Failures have been compensated and the control law for the rewritten system allowed to stabilize the system around the reference steady-state trajectory with sufficient precision. The deviations depend mainly on the fault compensation error in the steady-state. In a previous work (Sarotte et al. (2018)) a FTCS has been developed and tested on the same model, linearized around a steady state trajectory, with an EUIO for the fault estimation and an LQR for the system convergence and stability. The performances of those two methods can then be compared, see Table 5. The control law performances in terms of fault compensation and stability of the two control methods (EUIO-LQR and UUIO-MPC) are equivalent for the pressure regulation in the steady-state but the performances for the mass flow rate are increased with a factor ten. The control law allows to compensate for a failure in the transient and to track down a reference trajectory (see Figure 3). Since the system is not linearized around a steady-state reference in the case of the nonlinear FTCS, the stability domain is larger and the fault compensation error has less impact on the system performances.

Table 5. Deviations comparison EUIO+LQR / UUIO+MPC

Control simulation	Fault 1 in the transient	Deviations (%)
Pressure	UUIO - MPC	9.24e-2
	EUIO - LQR	1.08
Input mass flow rate	UUIO - MPC	0.13
	EUIO - LQR	0.35
Input pressure reference	UUIO - MPC	2.90e-2
	EUIO - LQR	1.23

5. CONCLUSION

In this paper a nonlinear FTC scheme has been proposed to ensure the stability of pressure and mass flow rates in the cooling circuit of a cryogenic test bench as well as to compensate for an additive actuator failure. Once the fault in the actuator has been detected by the FDI method composed of a first UUIO, the designed FTCS based on a fault estimator and a second UUIO permits to compensate for the failure and to converge if necessary to a chosen steady state. This FTCS consists in a MPC based on the minimization of an infinite horizon cost function and a direct fault compensation under the resolution of LMIs on an equivalent system where the unknown input is expressed as a function of the known state and known input vectors in order to decouple only the fault effect on the system. This method has been compared to a FTCS composed of an EUIO and a LQR controller and shows better performances for fault compensation and state reference tracking in the transients. Future work will address the design of a method to take into account the effect of input saturation, the limitation of overshoots and the validation of the developed FTCS on other part of the test bench facilities.

REFERENCES

Abbas-Turki, M., Duc, G., Clement, B., and Theodoulis, S. (2007). Robust gain scheduled control of a space launcher by introducing LQG/LTR ideas in the NCF robust stabilisation problem. In *46th IEEE Conference on Decision and Control*, 2393–2398.

Betta, G. and Pietrosanto, A. (2000). Instrument fault detection and isolation: State of the art and new research trends. *IEEE Transactions on Instrumentation and Measurement*, 49(1), 100–107.

Darouach, M., Zasadzinski, M., and Xu, S.J. (1994). Full-order observers for linear systems with unknown inputs. *IEEE Transactions on Automatic Control*, 39(3), 606–609.

Ding, S.X. (2008). *Model-based fault diagnosis techniques: design schemes, algorithms, and tools*. Springer Science & Business Media.

Gertler, J. (2013). *Fault detection and diagnosis*. Springer.

Ioannou, P.A. and Sun, J. (1996). *Robust adaptive control*, volume 1. PTR Prentice-Hall Upper Saddle River, NJ.

Johnson, D.M. (1996). A review of fault management techniques used in safety-critical avionic systems. *Progress in Aerospace Sciences*, 32(5), 415–431.

Józefowicz, R., Witczak, M., and Korbicz, J. (2011). Design of an unscented unknown input filter with interacting multiple model algorithm. In *19th Mediterranean Conference on Control & Automation (MED)*, 773–778.

Maciejowski, J. (1999). Modelling and predictive control: Enabling technologies for reconfiguration. *Annual reviews in Control*, 23, 13–23.

Magni, L., De Nicolao, G., Scattolini, R., and Allgöwer, F. (2003). Robust model predictive control for nonlinear discrete-time systems. *International Journal of Robust and Nonlinear Control: IFAC-Affiliated Journal*, 13(3-4), 229–246.

Mhaskar, P., Gani, A., and Christofides, P.D. (2006). Fault-tolerant control of nonlinear processes: performance-based reconfiguration and robustness. *International Journal of Robust and Nonlinear Control: IFAC-Affiliated Journal*, 16(3), 91–111.

Poursafar, N., Taghirad, H., and Haeri, M. (2010). Model predictive control of non-linear discrete time systems: a linear matrix inequality approach. *IET Control Theory & Applications*, 4(10), 1922–1932.

Sarotte, C., Marzat, J., Piet-Lahanier, H., Iannetti, A., Galeotta, M., and Ordonneau, G. (2018). Actuator fault tolerant system for cryogenic combustion bench cooling circuit. *IFAC-PapersOnLine*, 51(24), 592–599.

Theilliol, D., Join, C., and Zhang, Y. (2008). Actuator fault tolerant control design based on a reconfigurable reference input. *International Journal of Applied Mathematics and Computer Science*, 18(4), 553–560.

Vingert, L., Ordonneau, G., Fdida, N., and Grenard, P. (2015). A rocket engine under a magnifying glass. *AerospaceLab*, (11), 15.

Wan, E.A. and Van Der Merwe, R. (2000). The unscented Kalman filter for nonlinear estimation. In *IEEE Adaptive Systems for Signal Processing, Communications, and Control Symposium*, 153–158. IEEE.

Witczak, M. (2007). *Modelling and estimation strategies for fault diagnosis of non-linear systems: from analytical to soft computing approaches*, volume 354. Springer Science & Business Media.

Wu, J. (2005). Liquid-propellant rocket engines health-monitoring: a survey. *Acta Astronautica*, 56(3), 347–356.

Yang, H., Jiang, B., and Cocquempot, V. (2010). Fault tolerant control and hybrid systems. In *Fault Tolerant Control Design for Hybrid Systems*, 1–9. Springer.

Yin, S., Xiao, B., Ding, S.X., and Zhou, D. (2016). A review on recent development of spacecraft attitude fault tolerant control system. *IEEE Transactions on Industrial Electronics*, 63(5), 3311–3320.

Zhong, M., Xue, T., and Ding, S.X. (2018). A survey on model-based fault diagnosis for linear discrete time-varying systems. *Neurocomputing*, 306, 51–60.